Chaos, Solitons and Fractals 186 (2024) 115289

Contents lists available at ScienceDirect

Chaos, Solitons and Fractals

journal homepage: www.elsevier.com/locate/chaos

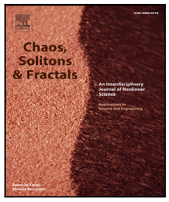

Adherence strategy based on evolutionary games in epidemic spreading

Meiling Xie [a], Ziyan Zeng [a], Yuhan Li [b], Minyu Feng [a,*]

[a] College of Artificial Intelligence, Southwest University, Chongqing, 400715, PR China
[b] School of Mathematical Sciences, Queen Mary University of London, London, UK

ARTICLE INFO

Keywords:
Epidemic spreading
Evolutionary game
Profit-driven decision-making
Conformity-driven decision-making
Adherence strategy

ABSTRACT

In light of the dynamic interaction between epidemic spreading and behavior responses, the development of a comprehensive epidemic model is both crucial and challenging. In this paper, based on the evolutionary game theory, we investigate the co-evolution of adherence strategy decision-making and epidemic spreading, with a particular focus on the role of conformity. Considering individual self-determination and population imitation, we analyze two distinct strategy updating rules: profit-driven decision-making and conformity-driven decision-making. We also account for the influence of neighbors' strategies on epidemic spread rates. Extensive simulations are conducted to analyze epidemic phase transitions and the distribution of infected individuals at the stationary state of the epidemic. By analyzing the adoption of strategies under different scenarios of conformity fractions, we find that conformity widens the disparity between different strategies over time. In conclusion, our results demonstrate that conformity promotes the adherence strategy, which helps reduce the size of the epidemic.

1. Introduction

In the context of recurrent epidemics, the decisions we make regarding our behavior can significantly impact the course of disease transmission. In response to the threat of infection, individuals may adopt behaviors that seek to control the spread of disease, such as self-protection [1], volunteer vaccination [2], social distancing [3], quarantine [4], and stay-at-home measures [5], which can reduce the risk of infection. The severity of an epidemic also impacts our decision-making in response, which is frequently neglected in most of the researches on the behavior during the epidemic. For instance, when the count of infected individuals is low, individuals may prioritize their own costs and benefits over the infection due to the losses in economic income, social opportunities, and convenience in daily life. Therefore, during the early stages of an outbreak or when the spread of the disease is not severe, individuals are not willing to adhere to prevention and control measures to preserve their daily routines. However, as the infection ratio rises, a larger fraction of the population tends to adhere strictly to guidelines and prioritize self-protection [6]. This dynamic can be understood through the lens of strategic decision-making principles explored in game theory, where players carefully balance personal payoff with the influence of their peers [7]. The efficacy of game-theoretic models in simulating complex decision-making mechanisms in the context of epidemics has been demonstrated by research findings [8].

The investigation of game theory on complex networks extends to the coupling of transmission dynamics and human decision-making processes in various fields [9,10]. As in many other areas of social life, the COVID-19 pandemic poses a public goods dilemma, e.g., if the majority of people cooperate, the larger group can defeat the virus [11]. Additionally, in the context of epidemic propagation, vaccination is modeled as a social public-goods dilemma among individuals considered as players [12]. In addition, a two-layered network paradigm has been devised to study the effect of information spreading [13]. Apart from the social distancing game [14], information about the current disease prevalence is assessed before decisions are made [15] as part of pay-off construction [16]. Typically, strategy updates involve players weighing their own fitness against that of their neighbors [17], thus considering different updating frequencies [18] and rules such as both learnings [19] and self-profit influencing vaccination behavior [20]. Similarly to rumor propagation, where profitability and herd psychology are considered, evolutionary game theory is used to construct the driving force mechanism of information [21]. To cover a comprehensive range of variables, a unified framework has been constructed to account for both long-term [8] and irrational decision-making processes [22]. Despite these advances, there is a need for more concise models that can effectively capture the dynamic interplay between the adoption of behaviors and the propagation of epidemics.

* Corresponding author.
E-mail address: myfeng@swu.edu.cn (M. Feng).

https://doi.org/10.1016/j.chaos.2024.115289
Received 19 May 2024; Received in revised form 23 June 2024; Accepted 11 July 2024

The field of game-theoretic decision-making in the dynamics of infectious disease has been extensively examined, employing stochastic methods on networks to capture the randomness and variability inherent in these processes. Initially, research concentrated on deterministic models with self-learning game settings, primarily focusing on mass human behavior. However, these early deterministic models, such as the compartment model, still fail to account for the heterogeneity of stochastic contacts among individuals [23]. To address the issue, more sophisticated models incorporate networks into epidemic modeling in order to capture different contact patterns [24] since networks are widely studied (e.g. random network [25], small-world network [26], scale-free network [27], multilayer network [28], high-order network [1], etc.). A graph-coupled hidden Markov model has been proposed for the study of stochastic transmission at the individual level [29], while the micro Markov Chain approach is used to derive the outbreak threshold of epidemics [28]. The compound Poisson process is also employed to model the epidemic progression [30]. With the introduction of queueing theory, the healthcare queueing system was optimized to minimize the infection rate [31]. An open Markov queueing system is employed to model the stochasticity of state transition in SIRS models [32]. On the other hand, non-repeated self-learning population games were widely studied in the early years. These models consider each individual to be perfectly rational, with complete information about the current epidemic prevalence and other individual's behaviors [33]. Another set of studies utilizes imitation to connect decision-making to a learning process that encompasses not only individuals but the entire population. For example, conformity-motivated susceptible individuals are influenced by both their neighbors and the population, illustrated by deterministic differential equations [20]. Based on Markov processes, the game transition is introduced to the game among network individuals [34]. Furthermore, myopic Markov perfect equilibrium is solved on a stochastic disease game to capture the self-interests of individuals [35].

The complex dynamics of decision-making are frequently observed in real-world epidemic transmission scenarios. However, existing disease models often inadequately capture these complexities [36]. The theoretical framework that thoroughly explores the interaction between these two aspects is significantly absent: the impact of behavioral patterns on disease spreading, and conversely, how disease transmission dynamics influence individual decision-making processes. To address these shortcomings, our study introduces a game-theoretic framework that integrates considerations of both individual self-determination and conformity-driven majority decisions. In particular, it considers the influence of both the conformity-driven decision-making process and the individual's own payoff and information. Moreover, the strategies selected by neighbors in turn influence the rate of epidemic spreading. The model emphasizes the significance of incorporating behavioral dynamics and social influences into epidemic modeling and intervention strategies.

The paper is structured as follows: In Section 2, we propose an epidemic spreading model coupled with the adherence strategy updating process. In Section 3, simulations are conducted to observe the effect of different system parameters on the epidemic size and analyze the role of conformity in strategy updating and epidemic spread. In Section 4, a summary of our findings and an outline of future work are concluded.

2. Adherence strategy in epidemic spread based on evolutionary game theory

In this paper, we introduce a novel network model that integrates two interrelated subprocesses: the propagation of an epidemic and the evolution of strategy responses. To facilitate a deeper understanding of epidemic propagation dynamics, we first elaborate on the formulation of the interactive payoffs between epidemic transmission and strategy selection by individuals, which offers a novel perspective on the investigation of epidemic dynamics. Then, we analyze the influence of the strategy on the rate of the epidemic spreading.

In order to illustrate the state and strategy of each individual within the network, we define every individual i by a two-dimensional stochastic process $\{X_i(t), Y_i(t)\}$, which presents the social behavior and health state of individual i at the discrete time t, respectively. More precisely, the social behavior of individual i is characterized by the stochastic process $X_i(t)$ with a state space $\mathcal{A} \in \{0, 1\}$, indicating whether individual i adheres to epidemic-prevention rules. In particular, the adherence strategy, indicated by $X_i(t) = 1$, signifies compliance with preventive and management measures, such as self-isolation. Conversely, the non-adherence strategy, demonstrated by behaviors like discarding these guidelines, is denoted by $X_i(t) = 0$. The health state $Y_i(t)$ assumes values from a discrete set of compartments denoted by $\mathcal{B}$. For example, choosing $\mathcal{B} \in \{S, I\}$ allows us to model the susceptible-infected-susceptible (SIS) epidemic process effectively.

2.1. Profit-driven strategy updating rule

In the context of an epidemic, the epidemic spreading within a network is largely influenced by whether individuals and their neighbors adhere to defense and control measures or not. The decision of each individual to comply with the rules depends on factors, including their own personal payoff and the size of the epidemic. Similarly to how players update their strategies in game theory, individuals tend to choose a particular strategy that offers a higher payoff. In a similar manner to how social factors and payoffs influence strategy selection, they also play a pivotal role in the spreading of an epidemic.

Therefore, the game theory provides an effective framework for modeling the spreading of epidemics. By representing individuals as vertices and their action choices as edges in a network, we can illustrate the process of updating strategies during an epidemic. Analogously, each individual within the network acts as a player in an evolutionary game, with the two possible actions for each susceptible individual, namely adhering or not adhering to control measures, corresponding to two distinct strategies.

The game strategy and fitness are governed by a two-player-two-strategy game. To begin, we establish the individuals' payoff matrix P as follows:

$$P = \begin{array}{c} \\ A \\ N \end{array} \begin{array}{c} \begin{array}{cc} A & N \end{array} \\ \begin{pmatrix} u_{aa} & u_{na} - c \\ u_{na} & u_{nn} \end{pmatrix} \end{array}, \tag{1}$$

where c denotes the cost associated with adherence, and $c > 0$. In the matrix, u_{na} represents the payoff when a non-adherer N interacts with an adherer A, and u_{aa} denotes the payoff when both individuals adhere, which includes the cost of adherence c. u_{nn} signifies the payoff when both individuals do not adhere. Additionally, when an adherer interacts with another non-adherer, there is a cost of c to adhere, resulting in a payoff of $u_{na} - c$. We assume that all payoffs are positive and normalized within the interval (0,1), i.e., $0 < u_{aa}, u_{na}, u_{nn} < 1$.

We then introduce two fitnesses, $\pi_i^0(t)$ and $\pi_i^1(t)$ for strategies, which represent a combination of sociopsychological, economic, and personal benefits obtained by individual i when adopting behaviors $X_i(t) = 0$ and $X_i(t) = 1$ at time t. Hence, the fitnesses $\pi_i^0(t)$, $\pi_i^1(t)$ for the non-adherer and the adherer respectively, are the total sum of payoffs from all neighbors, which are calculated as follows:

$$\begin{cases} \pi_i^0(t) = u_{na} \sum_{j \in \mathcal{V}} X_j(t) + u_{nn} \sum_{j \in \mathcal{V}} \left[1 - X_j(t)\right] \\ \pi_i^1(t) = u_{aa} \sum_{j \in \mathcal{V}} X_j(t) + (u_{na} - c) \sum_{j \in \mathcal{V}} \left[1 - X_j(t)\right], \end{cases} \tag{2}$$

where $\mathcal{V}$ includes all individuals connecting to individual i, and $X_j(t)$ denotes the strategy chosen by the neighbor j of individual i.

Based on the fitnesses, a susceptible individual i then autonomously determines whether to adopt the non-adherence strategy with a probability defined as

$$\mathbb{P}[X_i(t+1) = 0 | X_i(t) = 1] = \frac{\exp\{\pi_i^0(t)\}}{\exp\{\pi_i^1(t) N'(t)/[N'(t) - I(t)]\} + \exp\{\pi_i^0(t)\}}, \tag{3}$$

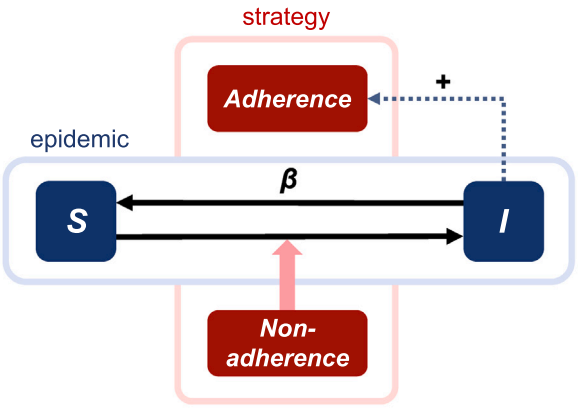

Fig. 1. Interactive influence between Strategy adoption and Epidemic spreading. The transmission dynamics of the SIS epidemic model are influenced by the choice of two strategies, adherence, or non-adherence. Specifically, opting for the non-adherence strategy leads to the infection of susceptible individuals, with β denoting the rate of being susceptible again. The symbol + indicates that the increase in the number of infected individuals prompts a greater number of individuals to adopt the adherence strategy.

where $I(t)$ indicates the count of infected individuals, and $N'(t)$ denotes the total population at time t. The probability is influenced by two factors: the fundamental payoffs and circumstantial information about the infection ratio based on the research [8]. With an increase in the number of infected individuals, there is a higher probability of strictly adhering to epidemic prevention and control measures. Conversely, when the infection count of individuals is low, the strategy selection is largely dependent on the fitnesses.

2.2. Conformity-driven strategy updating rule

Beyond the self-determination deliberations, individuals will not only weigh the fundamental payoffs but also adjust their decisions based on the majority choices made by their neighbors. The phenomenon is due to conformity, which is the tendency for individuals to follow their decisions with the majority choices of their neighbors, as illustrated in classic game theory [37].

In our model, individuals are assumed to possess knowledge of the strategies and status of their neighbors. Driven by conformity with the population, individuals are often influenced by their neighbors and the population. Hence, for an individual with $X_i(t) = 0$, if the majority of their neighbors choose the same strategy (i.e., non-adherence), then the strategy will be maintained with a higher probability. Conversely, if the majority of neighbors choose differently, the individual is likely to switch to the other strategy. The theoretical probability of a susceptible individual transferring its strategy is expressed as follows:

$$\mathbb{P}[X_i(t+1) = 1 | X_i(t) = 0] = \frac{1}{1 + \exp\left[\left(N_0 - k_h\right)/K\right]}, \tag{4}$$

where N_0 denotes the count of individuals who have adopted the same strategy as the individual i, while k_h denotes half the number of individual neighbors [20]. K quantifies the selection intensity to account for uncertainty in decision-making. In a similar way, we can get the probability of strategy transition from $X_i(t) = 1$ to $X_i(t+1) = 0$, by substituting N_0 with the count of adherers, which depicts the learning process of not only the neighbors but also the entire population.

2.3. Epidemic spreading process influenced by the strategy selection

The spreading of an epidemic is significantly influenced by the contact patterns among individuals and the strategies they adopt in response. When neighbors choose behavior strategies, it can greatly affect the infection rate. For simplicity, we assume that strict adherence to preventive measures grants complete protection and immunity against the contagious disease, implying that the individuals who adhere to rules remain unaffected by the epidemic during the given time step.

In the basic SIS model, an epidemic typically spreads pairwise from an infected individual, denoted as j to their neighbors with a probability $\alpha \in [0, 1]$. Based on the model, we incorporate the influence of strategies adopted by infected neighbors into our model. The probability that a susceptible individual i will become infected at time $t+1$ is given by

$$\mathbb{P}\left[Y_i(t+1) = I | Y_i(t) = S\right] = 1 - (1-\alpha)^{\sum_{j\in\mathcal{V}}[1 - X_j(t)]}, \tag{5}$$

where $\mathcal{V}$ is the set of individual j who are connected to individual i. The strategy adopted by neighbor j at time t is denoted by $X_j(t)$. In addition to contagion, each infected individual i recovers with probability $\beta \in (0, 1]$ at time step t, transitioning back to a susceptible again.

Fig. 1 illustrates the interrelationship between strategy selection and epidemic spreading in the model. In particular, the adoption of a non-adherence strategy affects the rate at which individuals transition from susceptible to infected states. Simultaneously, the real-time number of infected individuals dynamically influences the strategy selection of the population, with a higher prevalence of infections leading to a greater probability of adherence.

3. Simulation

In this section, we present the simulation results and analysis of our proposed game-theoretic epidemic model on the SIS model. Using the networkx packages in Python, we can observe the epidemic phase transition and the distribution of infected individuals at the stationary state under varying system parameters. Additionally, we analyze the adoption of strategies under two scenarios of conformity in different settings of the epidemic. To further investigate the role of conformity, we compare the epidemic sizes of two conformity scenarios with various system parameters, which allows us to detect the potential positive effect of promoting the adherence strategy.

3.1. Methods

The study uses a Watts-Strogatz (WS) small-world network comprising 4000 vertices. The network has an average degree of 10 and a rewiring probability of 0.7. In order to simulate different situations during an epidemic, we set various parameters as follows: The number of initially infected individuals denoted as $I(0) \in \{100, 800\}$, with the pairwise infection rate $\alpha \in \{0.035, 0.070, 0.140\}$ and the recovery rate $\beta \in \{0.005, 0.010, 0.015\}$. To start the simulation, about 100 vertices are selected to be infected, $I(0) = 100$ with $\alpha = 0.070$, $\beta = 0.010$. The selection intensity K is characterized by a value of $1/1000$.

With regard to the two strategy update rules, we define ρ_c as the proportion of individuals in the population motivated by conformity, implying that the proportion of profit-driven individuals is $1-\rho_c$, where $\rho_c \in \{0.1, 0.9\}$. Initially, ρ_c is set as 0.9, representing a situation with a high proportion of conformity-motivated individuals.

To simulate different situations during an epidemic, we define different values for the payoffs and the cost c, therefore three kinds of payoff matrices for adopting strategies are designed as follows,

- PM 1: $u_{aa} < u_{na} - c < u_{na} < u_{nn}$, $c = 0.02$.

$$P_1 = \begin{array}{c} \\ A \\ N \end{array} \begin{array}{c} \begin{array}{cc} A & N \end{array} \\ \begin{pmatrix} 0.01 & 0.03 \\ 0.05 & 0.1 \end{pmatrix} \end{array} \tag{6}$$

- PM 2: $u_{na} - c < u_{aa} = u_{na} < u_{aa}$, $c = 0.01$.

$$P_2 = \begin{array}{c} \\ A \\ N \end{array} \begin{array}{c} \begin{array}{cc} A & N \end{array} \\ \begin{pmatrix} 0.05 & 0.04 \\ 0.05 & 0.1 \end{pmatrix} \end{array} \tag{7}$$

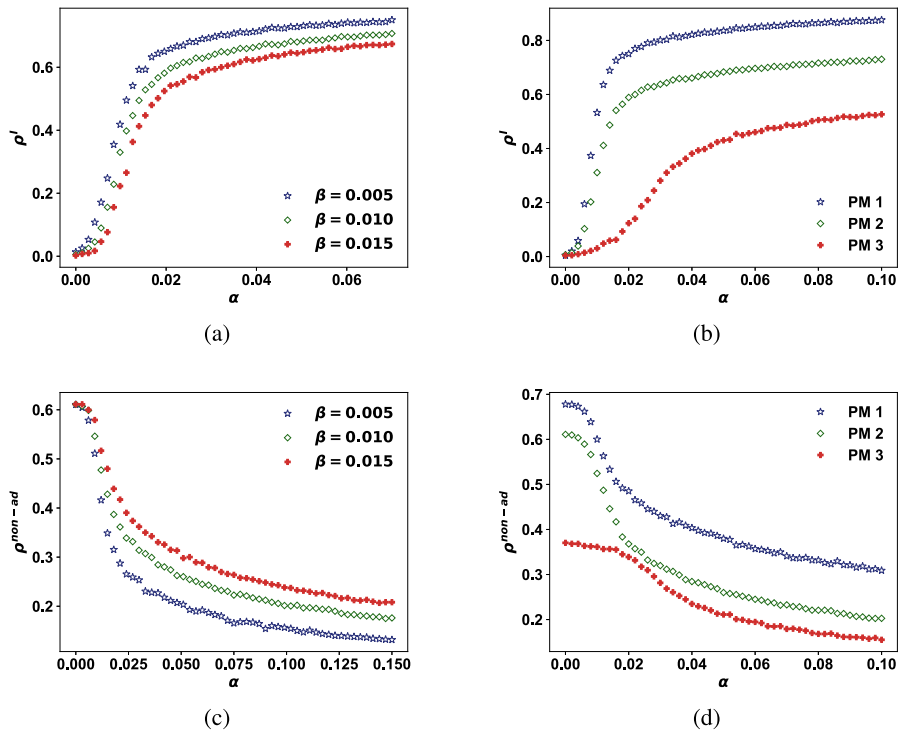

Fig. 2. Impact of the recovery rate β, the payoffs, and the per-contact infection rate α on the final epidemic size and the final size of the non-adherers. The spread size is characterized by the density of infected individuals in the stationary epidemic, denoted by ρ^{I}. The term, $\rho^{\mathrm{non-ad}}$ represents the proportions of susceptible non-adherers. (a) Final epidemic size ρ^{I} versus α for three distinct βs' values. (b) Final epidemic size ρ^{I} versus α for three payoff matrices. (c) $\rho^{\mathrm{non-ad}}$ at stationary epidemic versus α for three different βs' values. (d) $\rho^{\mathrm{non-ad}}$ at stationary epidemic versus α for three payoff matrices.

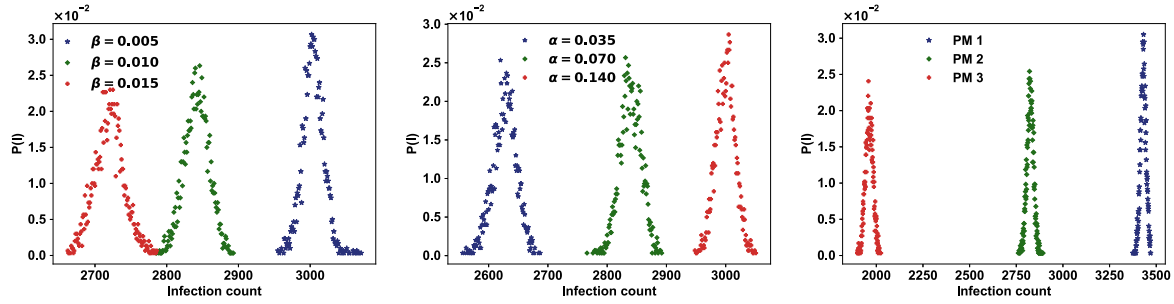

Fig. 3. Distribution of infected (I) individuals with different parameters at the stationary epidemic. The distribution of infection count is influenced by three distinct parameters. In Figs. 3(a)–3(c), the distributions are displayed with each parameter varied, including β, α, and the payoffs in order. (a) $\beta \in \{0.005, 0.010, 0.015\}$, $\alpha = 0.07$, with the payoff matrix PM 2. (b) $\alpha \in \{0.035, 0.070, 0.140\}$, $\beta = 0.01$, with the payoff matrix PM 2. (c) $\alpha = 0.07$, $\beta = 0.01$, with the payoff matrix PM 1, PM 2, and PM 3.

- PM 3: $u_{nn} < u_{na} - c < u_{na} < u_{aa}$, $c = 0.01$.

$$P_3 = \begin{array}{c} \\ A \\ N \end{array} \begin{array}{c} \begin{array}{cc} A & N \end{array} \\ \begin{pmatrix} 0.1 & 0.04 \\ 0.05 & 0.01 \end{pmatrix} \end{array} \tag{8}$$

The three payoff structures are based on experimental data to achieve a balance between the infection count and the strategy payoff.

3.2. The effect of parameters in the game-theoretic SIS model

The following simulations focus on the number of individuals in the infected state I in the stationary epidemic, denoted as ρ^{I}. Firstly, we demonstrate the epidemic phase transition of the infection counts under different parameters. Additionally, we present the distribution of the infection count at the stationary state when time is sufficiently extended, with the aim of obtaining the experimental expectation of it.

The system dynamics of the epidemic are governed by three parameters, namely the pairwise infection rate α, the recovery rate β, and the fitnesses $\pi_i^0(t)$ and $\pi_i^1(t)$. For the purpose of exploring the effect of parameters in our model, we analyze the final epidemic size ρ^{I} over a range of varying pairwise infection rates α in Fig. 2. More specifically, we vary the value of β in terms of epidemic transmission, as well as different payoff matrices in terms of strategy choice. For clarity, these results are presented using the quasi-stationary algorithm, as detailed in [38].

As illustrated in Figs. 2(a)–(b), it can be observed that the final infected ratio ρ^{I} consistently increases as α rises. In particular, Fig. 2(a) illustrates a sequential decrease in ρ^{I} for $\beta = 0.005$, $\beta = 0.010$, $\beta = 0.015$ with a fixed payoff matrix (PM 2), which indicates that a higher β contributes to a smaller epidemic size. Similarly, Fig. 2(b) demonstrates a corresponding trend where the final epidemic size ρ^{I} decreases sequentially as the payoff u_{aa} increases from payoff matrix

PM 1 to PM 3. The comparative advantages of the two strategies over time in the epidemic are reflected in the different values of payoffs. With a constant recovery rate $\beta = 0.010$, a higher u_{aa} correlates with a reduced epidemic size. Conversely, as illustrated in Figs. 2(c)–(d), an increase in α is accompanied by a reduction in $\rho^{\text{non-ad}}$. An increase in α results in a reduction in the number of susceptible individuals in the stationary epidemic. Meanwhile, more susceptible individuals adopt the adherence strategy, therefore $\rho^{\text{non-ad}}$ decreases. Analogously, as β increases, there is a corresponding decrease in $\rho^{\text{non-ad}}$, demonstrating the significance of enhancing the recovery rate in promoting adherence to the guidelines. As shown in Fig. 2(d), with the lowest value of u_{aa} and the highest c for PM 1 leads to the highest value of $\rho^{\text{non-ad}}$, which is attributed to the fact that as u_{aa} increases, fewer individuals adopt the non-adherence strategy, thereby influencing the final proportion of its adopters.

Nevertheless, in Fig. 2(d), there is a larger disparity between the red curves and the other two curves compared to Figs. 2(a)–(c). In particular, as α approaches 0, the three curves in Figs. 2(a)–(c) overlap. However, in Fig. 2(d), both the blue curve and green curve are above 0.6, while the red curve with PM 3 is around half, with a value between 0.3 and 0.4. The observed pattern can be attributed to the fact that when the infection count is low, a greater proportion of individuals tend to adopt the non-adherence strategy, and the probability is largely dependent on the fitnesses. In the payoff matrix, the payoffs for non-adherers u_{na} and u_{nn} are identical, but $u_{na} < u_{nn}$. As a result, the blue and green curves are close, and $\rho^{\text{non-ad}}$ exhibits a higher level of adoption. However, in PM 3, where the payoff $u_{na} > u_{nn}$, more susceptible individuals are inclined to adopt the adherence strategy.

Furthermore, we investigate the expectation of infection count under different parameter values in the dynamic system, as illustrated by our experiments in Fig. 3. In Fig. 3(a), the broader distribution denoted by green triangles contrasts with the narrower blue distribution, while the red scatter plot, indicating the highest variance, extends the farthest. Specifically, the red distribution has a standard deviation of 20.74, while the other distributions have standard deviations of 17.36 and 14.77, respectively. Notably, the blue scatter plot, corresponding to the recovery rate $\beta = 0.005$, is positioned on the right with its mode of 3004. In contrast, the red distribution, which corresponds to the highest recovery rate, is positioned towards the left, with a mean value of 2720. The green scatter plot, reflecting an intermediate recovery rate, is positioned between the other two distributions, with a mean value of 2842, which suggests that a lower β corresponds to a higher count of infected individuals and a more pronounced peak in the distribution. In Figs. 3(b)–(c), the differences in mode and peak are relatively minor. In detail, the expectation value of the distribution with $\alpha = 0.07$, marked by the green triangles, is 2839, whereas the distribution with double the α value has a peak near 3000. In contrast, the distribution with $\alpha = 0.035$, depicted by blue stars, exhibits a peak value of 2627, which reveals a contrasting relationship between the distribution and the parameter α, in contrast to β. In Fig. 3(c), the distribution with PM 1 is positioned on the rightmost side of the graph, where the peak value is near 3430. The distribution with PM 3, whose expected value is approximately 1962, is situated on the leftmost side, indicating that a lower payoff u_{aa} and a higher adherence cost c correspond to a higher count of infected individuals. The distribution corresponding to PM 2 has an expected value of around 2824, which indicates the steady-state infection count in the experiment when using PM 2, with $\alpha = 0.07$, and $\beta = 0.010$ in our model.

3.3. Time evolution of epidemic and strategy selection

In addition to analyzing the impact of the various parameters, we also explore the role of conformity. We observe the time evolution of individual strategy ratio and infection ratio with two different values of conformity-driven fraction ρ_c in 40 iterations, which are depicted in Fig. 4.

To simulate different epidemic situations, in the two conformity scenarios, we respectively set two different initial counts of infected individuals $I(0)$. Figs. 4(a)–(b) present a context favorable to the non-adherence strategy, with $I(0) = 100$ and PM 1. In such a setting, a significantly larger fraction of the population opts for the non-adherence strategy due to the higher payoff of the adherence strategy and a higher cost of adherence. As the progression of the epidemic, the infected ratios increase, which are depicted as green dashed lines. Therefore, a general decline in both $\rho^{\text{non-ad}}$, represented by the red diagram, and ρ^{ad}, illustrated by the blue diagrams, is observed due to the reduction of susceptible population. However, the non-adherers ratio is higher than the adherers ratio during the initial phase of the epidemic. At this stage, the number of infected individuals is relatively low, and the higher payoff for non-adherence u_{nn} in PM 2 leads to an increased prevalence of non-adherence in our model. As the ratio of infected individuals increases, the adherers surpass the non-adherers count.

Conversely, with $I(0) = 800$ and PM 3 in Figs. 4(c) and (d), the epidemic conditions are more conducive to the adherence strategy. Consequently, the proportion of adherers, represented by the blue curve, is always greater than that of individuals who do not adhere, as depicted by the red curves.

The introduction of a high conformity fraction serves to accentuate the divergence in strategy adoption between the two conformity scenarios. Specifically, in Figs. 4(a) and (b), the dominance of the non-adherence strategy gives rise to a greater number of non-adherers as a consequence of conformity, thereby widening the gap between the each other. A similar observation can be made when comparing Figs. 4(c) and (d). Even in the stationary state of the epidemic where the adherers exceed the non-adherers, the disparity in Fig. 4(c) with $\rho_c = 0.9$ is greater than in Fig. 4(d) with $\rho_c = 0.1$. In the scenario where the adherence strategy is favored, the adoption of this strategy is more prevalent in the early stages of the epidemic. Consequently, conformity encourages greater adoption of the adherence strategy, which leads to a greater disparity in the number of adherers compared to non-adherers. As the number of infections increases, the adoption of the non-adherence strategy decreases.

In order to visually examine the relationship between the density of non-adherence individuals, $\rho^{\text{non-ad}}$ and the infection count, we analyze their temporal variation depicted in Figs. 4(e)–(h), after repeated simulations. In all four figures, the curves exhibit a general decline, indicating that as the infection ratio increases, $\rho^{\text{non-ad}}$ decreases, which is consistent with our theory.

In the situation favoring the non-adherence strategy in Figs. 4(e)–(f), we note a transient increase in $\rho^{\text{non-ad}}$ when the infected ratios are close to 0, which results from, at the beginning of the epidemic, the infected ratio is low, leading to fewer individuals adhering to guidelines. However, the increase is more pronounced in Fig. 4(e), which depicts the scenario with a high conformity fraction $\rho_c = 0.9$, compared to Fig. 4(b). A higher fraction of the conformity-driven population leads to more individuals adopting the mainstream non-adherence strategy. This occurs despite the continuing, but relatively insignificant, rise in infections. On the contrary, in Fig. 4(g), there is a sharp decline in $\rho^{\text{non-ad}}$ when the infection ratio is low. In the scenario with the relatively high infection ratio and the superior payoff of adherence which favors the adherence strategy, adherence becomes the dominant strategy, with a greater number of individuals conforming to it.

3.4. Stationary state of epidemic and strategy selection under two conformity scenarios

For the purpose of gaining further insight into the role of conformity in epidemic dynamics, we perform a comparative analysis of the final epidemic size, denoted as ρ^{I}, across different conformity scenarios in Fig. 5. First, the stationary infection ratio ρ^{I}, is examined as a function

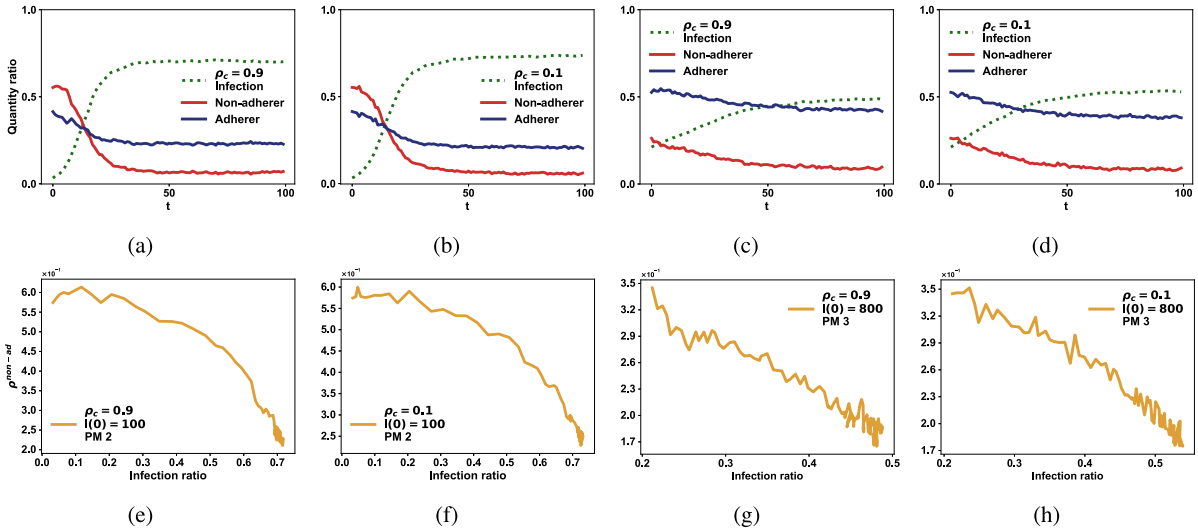

Fig. 4. Time evolution of the epidemic spreading and strategy selection under four scenarios. The progression of the epidemic is characterized by the densities of infected individuals, susceptible adherers ρ^{ad}, and susceptible non-adherers $\rho^{\mathrm{non-ad}}$. In panels (a)–(d), we display the temporal infection ratio in green, $\rho^{\mathrm{non-ad}}$ in red, and ρ^{ad} in blue. Panels (e)–(h) illustrate the corresponding ratio of non-adherers $\rho^{\mathrm{non-ad}}$, as the infection count changes over time. Different scenarios are represented across panels. (a) and (c) illustrate strategy updates in a scenario with a high conformity fraction $\rho_c = 0.9$, whereas (b) and (d) depict strategy updates with a low conformity fraction $\rho_c = 0.1$. (a)–(b), and (e)–(f) depict scenarios with the initially infection count $I(0) = 100$ and PM 2, which favors non-adherence strategy. (c)–(d), and (g)–(h) represent situations favoring adherence strategy with the initially infection count $I(0) = 800$ and PM 3. (For interpretation of the references to color in this figure legend, the reader is referred to the web version of this article.)

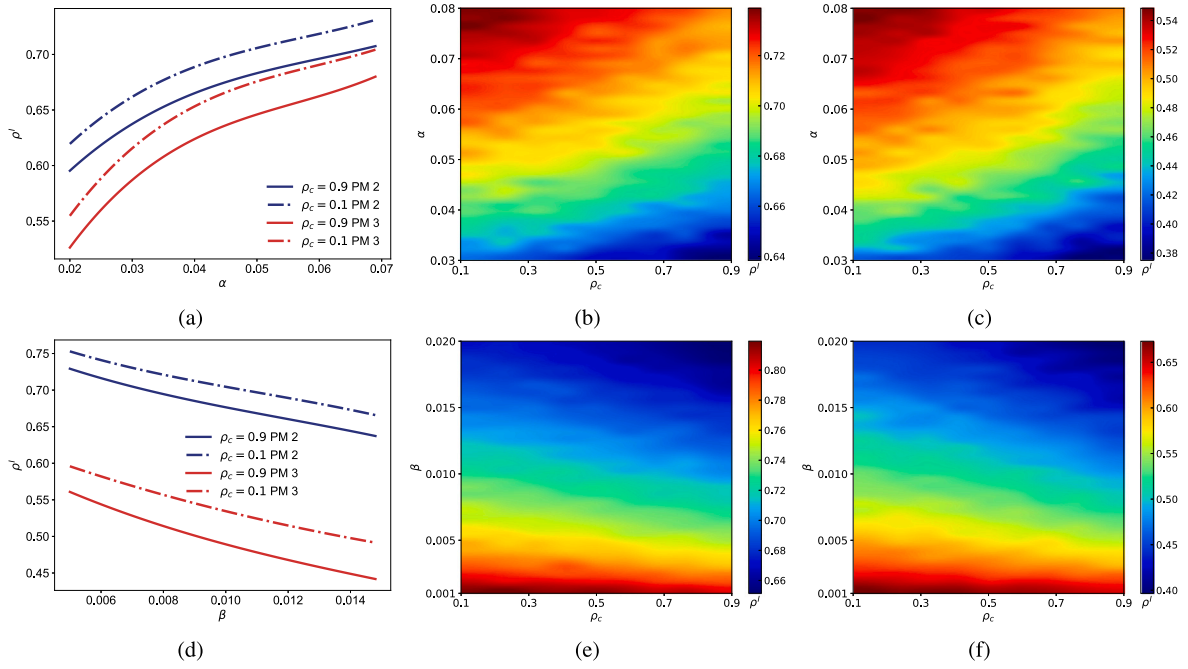

Fig. 5. The impact of conformity on the final epidemic size ρ^I in two situations with varying system parameters. In (a) and (d), the solid curves denote situations with a high conformity fraction $\rho_c = 0.9$, while dashed curves denote the situations with a low conformity fraction $\rho_c = 0.1$. The blue curves indicate PM 2 with $I(0) = 100$, while the red curves indicate PM 3 with $I(0) = 800$. The curves are fitted to the data with polynomial three-order fitting techniques in order to facilitate comparison. We vary the conformity fraction ρ_c under different values of α ((b)–(c)) and β ((e)–(f)) to observe their impact on the epidemic size ρ^I. To facilitate comparison, the following values are used for the initial settings: PM 2 with $I(0) = 100$ for (b) and (e), PM 3 with $I(0) = 800$ for (c) and (f). (For interpretation of the references to color in this figure legend, the reader is referred to the web version of this article.)

of the pairwise infection rate α and the recovery rate β in four scenarios, which is depicted in Figs. 5(a) and (d). In particular, we consider two values of ρ_c, specifically $\rho_c = 0.1$ and $\rho_c = 0.9$, each with different initial conditions for the payoff matrix and $I(0)$. Figs. 5(b) and (e) display the situation in PM 2 with $I(0) = 100$, while Figs. 5(d) and (f) show the situation in PM 3 with $I(0) = 800$. To present our comparative findings more clearly, we employ polynomial three-order fitting techniques to generate curves representing the empirical trends.

In Figs. 5(a) and (d), the blue curves representing PM 2 consistently lie above the red curves denoting PM 3, which is attributed to the fact that PM 2 promotes non-adherence, consequently amplifying the epidemic size. Notably, the disparity between the dashed red curve and the solid red curve is consistently greater than that observed for the blue curves. In PM 3 with the highest value of u_{nn}, adherence is dominant, and a high conformity fraction prompts more individuals to adopt an adherence strategy.

Figs. 5(b)–(c), (e)–(f) illustrate a detailed analysis of how the stationary infection ratio ρ^{I} varies with changes in the conformity fraction, clarifying the impact of various parameters and conformity on the epidemic spreading. Specifically, as we increase α and decrease β, the epidemic size ρ^{I} diminishes. Moreover, an increase in ρ_c leads to a decrease in ρ^{I}, demonstrating the positive impact of conformity on epidemic control. This is because conformity promotes adherence strategy in the late stages of the epidemic, thereby highlighting the significant role it plays in epidemic control and management.

4. Conclusions and outlooks

In this study, we investigate the complex dynamics between strategic decision-making and epidemic propagation. Specifically, our novel model integrates an epidemic-spreading mechanism with a dynamic adherence strategy updating process. Taking into account individual self-determination, including information and payoff related to the epidemic, as well as the imitation of the population due to conformity, we analyzed two strategy updating rules: profit-driven decision-making and conformity-driven decision-making. In terms of the epidemic spread, we consider the impact of neighboring strategies on the infected probability. Through extensive simulations, we explore the effect of various system parameters and obtain the expected number of infected individuals from the experiments. Under four different scenarios, the evolution of the epidemic over time demonstrates how conformity widens the disparity between the two strategies. Further simulations are carried out to explore the effect of conformity on the epidemic size, revealing that conformity promotes the adherence strategy, thereby positively diminishing disease spread size.

Future research could be directed toward refining the model to account for varying levels of conformity, including partial conformity across diverse populations. Additionally, individuals could be depicted as adopting strategies based on a comprehensive consideration of both aspects, rather than a unilateral consideration. It would be beneficial to explore the impact of additional social factors on strategy adoption, such as rationality and risk perception. Furthermore, the model could be expanded to simulate the SIR (Susceptible–Infected–Recovered) and other epidemic models in order to enhance its predictive power and applicability to actual epidemic containment strategies. Further simulations could also assist in understanding the thresholds and conditions that give rise to significant changes in epidemic dynamics.

CRediT authorship contribution statement

Meiling Xie: Writing – review & editing, Writing – original draft, Resources, Methodology, Conceptualization. **Ziyan Zeng:** Writing – review & editing, Visualization, Methodology, Conceptualization. **Yuhan Li:** Visualization, Supervision, Methodology. **Minyu Feng:** Visualization, Supervision, Resources, Funding acquisition.

Declaration of competing interest

The authors declare that they have no known competing financial interests or personal relationships that could have appeared to influence the work reported in this paper.

Data availability

Data will be made available on request.

Acknowledgments

This work was supported by the National Natural Science Foundation of China (NSFC) under Grant No. 62206230, the Natural Science Foundation of Chongqing, PR China under Grant No. CSTB2023NSCQ-MSX0064, and Graduate Research Innovation Project of Southwest University, PR China under Grant No. SWUS24190.

References

[1] Liu L, Feng M, Xia C, Zhao D, Perc M. Epidemic trajectories and awareness diffusion among unequals in simplicial complexes. Chaos Solitons Fractals 2023;173:113657.
[2] Krueger T, Gogolewski K, Bodych M, Gambin A, Giordano G, Cuschieri S, et al. Risk assessment of COVID-19 epidemic resurgence in relation to SARS-CoV-2 variants and vaccination passes. Commun Med 2022;2(1):23.
[3] Gosak M, Kraemer MU, Nax HH, Perc M, Pradelski BS. Endogenous social distancing and its underappreciated impact on the epidemic curve. Sci Rep 2021;11(1):3093.
[4] Chen J, Xia C, Perc M. The SIQRS propagation model with quarantine on simplicial complexes. IEEE Trans Comput Soc Syst 2024;1–12.
[5] Aronna M, Guglielmi R, Moschen L. A model for COVID-19 with isolation, quarantine and testing as control measures. Epidemics 2021;34:100437. http://dx.doi.org/10.1016/j.epidem.2021.100437.
[6] Lucchini L, Centellegher S, Pappalardo L, Gallotti R, Privitera F, Lepri B, et al. Living in a pandemic: changes in mobility routines, social activity and adherence to COVID-19 protective measures. Sci Rep 2021;11(1):24452.
[7] Allen B, Lippner G, Chen Y-T, Fotouhi B, Momeni N, Yau S-T, et al. Evolutionary dynamics on any population structure. Nature 2017;544(7649):227–30.
[8] Ye M, Zino L, Rizzo A, Cao M. Game-theoretic modeling of collective decision making during epidemics. Phys Rev E 2021;104(2):024314.
[9] Shen S, Li H, Han R, Vasilakos AV, Wang Y, Cao Q. Differential game-based strategies for preventing malware propagation in wireless sensor networks. IEEE Trans Inf Forensics Secur 2014;9(11):1962–73.
[10] Feng M, Zeng Z, Li Q, Perc M, Kurths J. Information dynamics in evolving networks based on the birth-death process: Random drift and natural selection perspective. IEEE Trans Syst Man Cybern: Syst 2024.
[11] Capraro V, Boggio P, Böhm R, Perc M, Sjåstad H, Miller M. Cooperation and acting for the greater good during the COVID-19 pandemic. In: The social science of the COVID-19 pandemic: A call to action for researchers. Oxford University Press Oxford; 2021.
[12] Liu T, Li P, Chen Y, Zhang J. Community size effects on epidemic spreading in multiplex social networks. PLoS One 2016;11(3):e0152021.
[13] Kabir KA, Kuga K, Tanimoto J. The impact of information spreading on epidemic vaccination game dynamics in a heterogeneous complex network-a theoretical approach. Chaos Solitons Fractals 2020;132:109548.
[14] Poletti P, Caprile B, Ajelli M, Pugliese A, Merler S. Spontaneous behavioural changes in response to epidemics. J Theoret Biol 2009;260(1):31–40.
[15] Feng M, Li X, Li Y, Li Q. The impact of nodes of information dissemination on epidemic spreading in dynamic multiplex networks. Chaos 2023;33(4).
[16] Funk S, Salathé M, Jansen VA. Modelling the influence of human behaviour on the spread of infectious diseases: A review. J R Soc Interface 2010;7(50):1247–56.
[17] Wang C, Zhu W, Szolnoki A. The conflict between self-interaction and updating passivity in the evolution of cooperation. Chaos Solitons Fractals 2023;173:113667.
[18] Mao Y, Rong Z, Xu X, Han Z. Influence of diverse timescales on the evolution of cooperation in a double-layer lattice. Front Phys 2023;11:1272395.
[19] Shi Y, Rong Z. Analysis of Q-learning like algorithms through evolutionary game dynamics. IEEE Trans Circuits Syst II 2022;69(5):2463–7.
[20] Wang X, Jia D, Gao S, Xia C, Li X, Wang Z. Vaccination behavior by coupling the epidemic spreading with the human decision under the game theory. Appl Math Comput 2020;380:125232.
[21] Xiao Y, Chen D, Wei S, Li Q, Wang H, Xu M. Rumor propagation dynamic model based on evolutionary game and anti-rumor. Nonlinear Dynam 2019;95:523–39.
[22] Li X, Han W, Yang W, Wang J, Xia C, Li H-j, et al. Impact of resource-based conditional interaction on cooperation in spatial social dilemmas. Phys A 2022;594:127055.
[23] Li X, Hao G, Zhang Z, Xia C. Evolution of cooperation in heterogeneously stochastic interactions. Chaos Solitons Fractals 2021;150:111186.
[24] Cliff OM, Harding N, Piraveenan M, Erten EY, Gambhir M, Prokopenko M. Investigating spatiotemporal dynamics and synchrony of influenza epidemics in Australia: An agent-based modelling approach. Simul Model Pract Theory 2018;87:412–31.
[25] Rong Z, Wu Z-X, Li X, Holme P, Chen G. Heterogeneous cooperative leadership structure emerging from random regular graphs. Chaos 2019;29(10).
[26] Watts DJ, Strogatz SH. Collective dynamics of 'small-world'networks. Nature 1998;393(6684):440–2.
[27] Mao Y, Rong Z, Wu Z-X. Effect of collective influence on the evolution of cooperation in evolutionary prisoner's dilemma games. Appl Math Comput 2021;392:125679.
[28] Fan J, Yin Q, Xia C, Perc M. Epidemics on multilayer simplicial complexes. Proc R Soc A 2022;478(2261):20220059.
[29] Dong W, Pentland A, Heller KA. Graph-coupled HMMs for modeling the spread of infection. 2012, arXiv preprint arXiv:1210.4864.
[30] Xie M, Li Y, Feng M, Kurths J. Contact-dependent infection and mobility in the metapopulation SIR model from a birth–death process perspective. Chaos Solitons Fractals 2023;177:114299.

[31] Alipour-Vaezi M, Aghsami A, Jolai F. Prioritizing and queueing the emergency departments' patients using a novel data-driven decision-making methodology, a real case study. Expert Syst Appl 2022;195:116568.
[32] Li Y, Zeng Z, Feng M, Kurths J. Protection degree and migration in the stochastic SIRS model: A queueing system perspective. IEEE Trans Circuits Syst I Regul Pap 2021;69(2):771–83.
[33] Bauch CT, Earn DJ. Vaccination and the theory of games. Proc Natl Acad Sci 2004;101(36):13391–4.
[34] Feng M, Pi B, Deng L-J, Kurths J. An evolutionary game with the game transitions based on the Markov process. IEEE Trans Syst Man Cybern: Syst 2023.
[35] Eksin C, Shamma JS, Weitz JS. Disease dynamics in a stochastic network game: A little empathy goes a long way in averting outbreaks. Sci Rep 2017;7(1):44122.
[36] Jusup M, Holme P, Kanazawa K, Takayasu M, Romić I, Wang Z, et al. Social physics. Phys Rep 2022;948:1–148.
[37] Chang SL, Piraveenan M, Pattison P, Prokopenko M. Game theoretic modelling of infectious disease dynamics and intervention methods: A review. J Biol Dyn 2020;14(1):57–89.
[38] Cator E, Van Mieghem P. Second-order mean-field susceptible-infected-susceptible epidemic threshold. Phys Rev E 2012;85:056111.